Measurement for Thermal Effusivity of $Al_xGa_{1-x}N$ Alloys Using Thermoreflectance with Periodic Heating

Hiroyuki Shibata[1], Hiromichi Ohta[2], Takashi Nemoto[3], Shun Nagayama[3], Yoshio Waseda[1], Katsushi Fujii[4] and K.Thomas Jacob[5]

[1]*Institute of Multidisciplinary Research for Advanced Materials, Tohoku University, 2-1-1 Katahira Aoba-ku Sendai, 980-8577, Japan*
[2]*Faculty of Engineering, Ibaraki University, 4-12-1 Nakanarisawamachi, Hitachi, 316-8511, Japan*
[3]*Graduate School of Engineering, Ibaraki University, 4-12-1 Nakanarisawamachi, Hitachi, 316-8511, Japan*
[4]*Center for Interdisciplinary Research, Tohoku University, Aramaki aza Aoba 6-3, Aoba-ku, Sendai, 980-8578, Japan*
[5]*Department of Materials Engineering, Indian Institute of Science, Bangalore 560 012, India*

(Received April 16, 2010 ; Final form May 31, 2010)

ABSTRACT

$Al_xGa_{1-x}N$ alloys with x=0.375, 0.398, 0.401, 0.592 and 0.696 were deposited on sapphire substrate by the hydride-vapor-phase epitaxy (HVPE) method. Thermal effusivity measurements were carried out on $Al_xGa_{1-x}N$ alloys using a thermal microscope at room temperature. The lag between a sinusoidal heating laser wave and thermoreflectance wave was used to measure the thermal diffusivity. Thermal conductivity values of the $Al_xGa_{1-x}N$ alloys were also obtained as a function of AlN mole fraction in the alloy. The thermal conductivity was found to decrease with increasing AlN fraction and the experimental data agree with values estimated using the virtual crystal model.

*Corresponding author: Hiroyuki Shibata e-mail address: shibata@tagen.tohoku.ac.jp
tel: +81-22-217-5161, fax: +81-22-217-5162
[1] waseda@tagen.tohoku.ac.jp
[2] ohta@mx.ibaraki.ac.jp
[4] k.fujii@cir.tohoku.ac.jp
[5] katob@materials.iisc.ernet.in

Keywords: AlGaN alloys, thermal effusivity, thermal conductivity, thermal microscope

1. INTRODUCTION

Wide band gap group III nitride AlN has been attracting attention as a promising material for use in heterostructure field-effect transistors (HFETs) embedded in high-temperature, high-power and high-frequency devices. Saura et al. /1/ have indicated that thermal management in high-power AlGaN/GaN heterojunction field-effect transistor devices is an important issue in the design and operation of devices. Large temperature increase in small device dimensions has been reported. In order to develop a model for efficient thermal management, a more detailed knowledge of self-heating effects, thermal properties of various materials used in producing the device, and interfacial heat resistance at heterojunctions is required.

Temperature distribution in the devices has been investigated using micro-Raman spectroscopy /2/ and photo luminescence method /3/. The temperature distribution is influenced by heat generation in the devices as well as heat extraction from the devices. Heat

extraction is strongly related to thermal conductivity of nitride materials.

The values of thermal conductivity of GaN are strongly affected by factors such as crystalinity, impurity concentration and dislocation density. Recently, a value of 253 W/(m·K) was reported for thermal conductivity of GaN /4/. The thermal conductivity of AlN was also reported /5/. However, information on thermal conductivity of the mixed nitride AlGaN is very limited. Daly et al. /6/ measured thermal conductivity of $Al_xGa_{1-x}N$ by the optical pump and probe technique. Liu and Balandian /7/ systematically investigated thermal conductivity of $Al_xGa_{1-x}N$ by the differential 3ω technique. The results indicate that the thermal conductivity of $Al_xGa_{1-x}N$ decreases with increasing Al content from x=0.0 to 0.4 with a positive temperature dependence. In order to reduce the uncertainty associated with the thermal management model for AlGaN/GaN high electron mobility transistor (HEMT), accurate values for thermal properties of AlGaN alloy are useful.

It is difficult to grow large-size samples of $Al_xGa_{1-x}N$ in the laboratory and the grown samples often show spatial distribution of physical properties. For measuring the local coefficient of heat transfer, good time resolution and a non-contact measurement technique are essential to reduce the influence of the surrounding area. Thermoreflectance method relies on detecting small temperature-dependent changes in reflection. The thermally induced change in the reflection coefficient can be detected as the optical reflection intensity of the temperature probe laser by a photodiode. Time resolution of thermoreflectance method is significantly better than those of thermocouples, resistance temperature sensors and radiation thermometers. Thermoreflectance is well suited for two-dimensional surface thermography of optically smooth, highly reflective materials that have a strong thermo-optic response. /6, 8-11/. Since a thermal microscope (hereafter referred to as TM) has been developed by combining the thermoreflectance method with a periodic heating system, the thermoreflectance method can be readily used /12-16/.

The purpose of this work is to report the thermal effusivity measurements for the $Al_xGa_{1-x}N$ alloy prepared by HVPE (hydride vapor phase epitaxy) using TM. Thermal effusivity of a material is defined as the square root of the product of the thermal conductivity and volumetric heat capacity ($b=\sqrt{\lambda\rho C_P}$). It is a measure of the materials ability to exchange thermal energy with its surroundings. It is related to thermal conductivity and thermal diffusivity:

$$b=\sqrt{\lambda\rho C_P}=\sqrt{\alpha}\rho C_P \quad (1)$$

where λ, C_P, ρ and α are thermal conductivity, specific heat capacity, mass density and thermal diffusivity, respectively. It is useful to recall that the heat capacity per unit volume, ρC_p , at room temperature lies within a small range around 2×10^6 J m^{-3} K^{-1} for a variety of solid materials /17/. Hence, the thermal effusivity value is very useful to estimate heat conducting property of materials. Thin film sample is usually grown on a substrate and it is difficult to separate the film from the substrate. Therefore, thermal transport property of the film sample is obtained from local measurements of temperature response of the sample surface unaffected by the substrate.

2. EXPERIMENTAL PROCEDURE

2.1 Sample

The $Al_xGa_{1-x}N$ alloy sample, 440 μm thick, was deposited by HVPE /18/ on a sapphire substrate. Mole fraction of AlN was measured by X-ray diffraction measurement of the lattice constant of the sample at five positions as shown in **Figure 1**. The five points are identified as top, bottom, right, left and middle, respectively. Each point was about 20 mm away from other points. The values of mole fraction of AlN measured at five positions are summarized in **Table 1**. There is composition variation across the nitride film. By making local measurements of thermal effusivity on the film, composition dependence of thermal properties are obtained. Smoothness of the deposited sample surface was insufficient for thermal effusivity measurements by TM. Therefore, the surface of the deposited $Al_xGa_{1-x}N$ alloy sample was polished. The

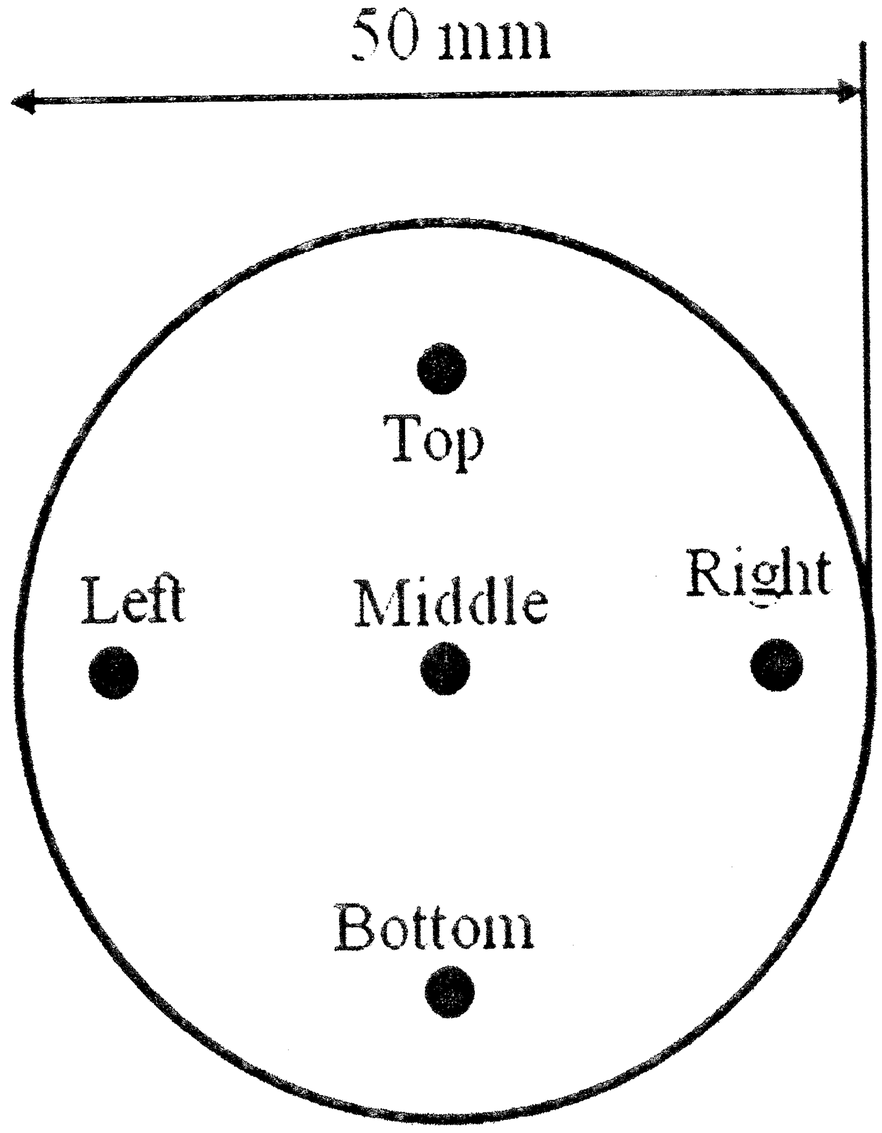

Fig. 1: Locations on the surface of $Al_xGa_{1-x}N$ sample used for measurements.

Table 1
AlN concentration at different locations on the sample surface.

Position	AlN mol%
Top	69.6
Middle	59.2
Bottom	37.5
Left	40.1
Right	39.8

maximum roughness of the polished sample surface of $Al_xGa_{1-x}N$ alloy sample was below 1 μm, the root-mean-square roughness was below 0.2 μm and arithmetical mean roughness was below 10 nm. The thermal effusivity measurements for the $Al_xGa_{1-x}N$ alloy samples were made by TM at the five points at which compositions were determined. In order to enhance the reliability of the results, the measurements were repeated 3 times at each point.

2.2 Principal of thermal microscope and apparatus

Since the procedure for measuring the thermal effusivity of a film sample by thermal microscope has already been described in detail elsewhere /12,13/, only a few essential points will be presented here. Schematic diagram of the experimental apparatus is shown in **Figure 2.** In this method, a small area of the sample surface is heated by an intensity-modulated laser beam and the temperature response is monitored using another laser beam based on thermoreflectance. Thermal effusivity is derived from the phase lag between the thermal wave and thermoreflectance signal. In order to improve the signal to the noise ratio in the thermoreflectance measurement, a molybdenum thin layer 100 nm in thickness is sputtered on the $Al_xGa_{1-x}N$ alloy sample. This molybdenum thin layer functions both as laser beam reflector for temperature measurement and as heat absorber. The profile of the temperature response is found to be unchanged by this molybdenum coating /12,13 /.

Two laser diodes are used with the beams coaxially aligned and focused on the sample surface. A compensating network based on a differential scheme is used for reducing the fluctuation caused by the instability of the laser diodes. Diameters of heating and detection areas are 23.4 μm and 7.2 μm, respectively /13/. A larger area is required to be heated by the heating

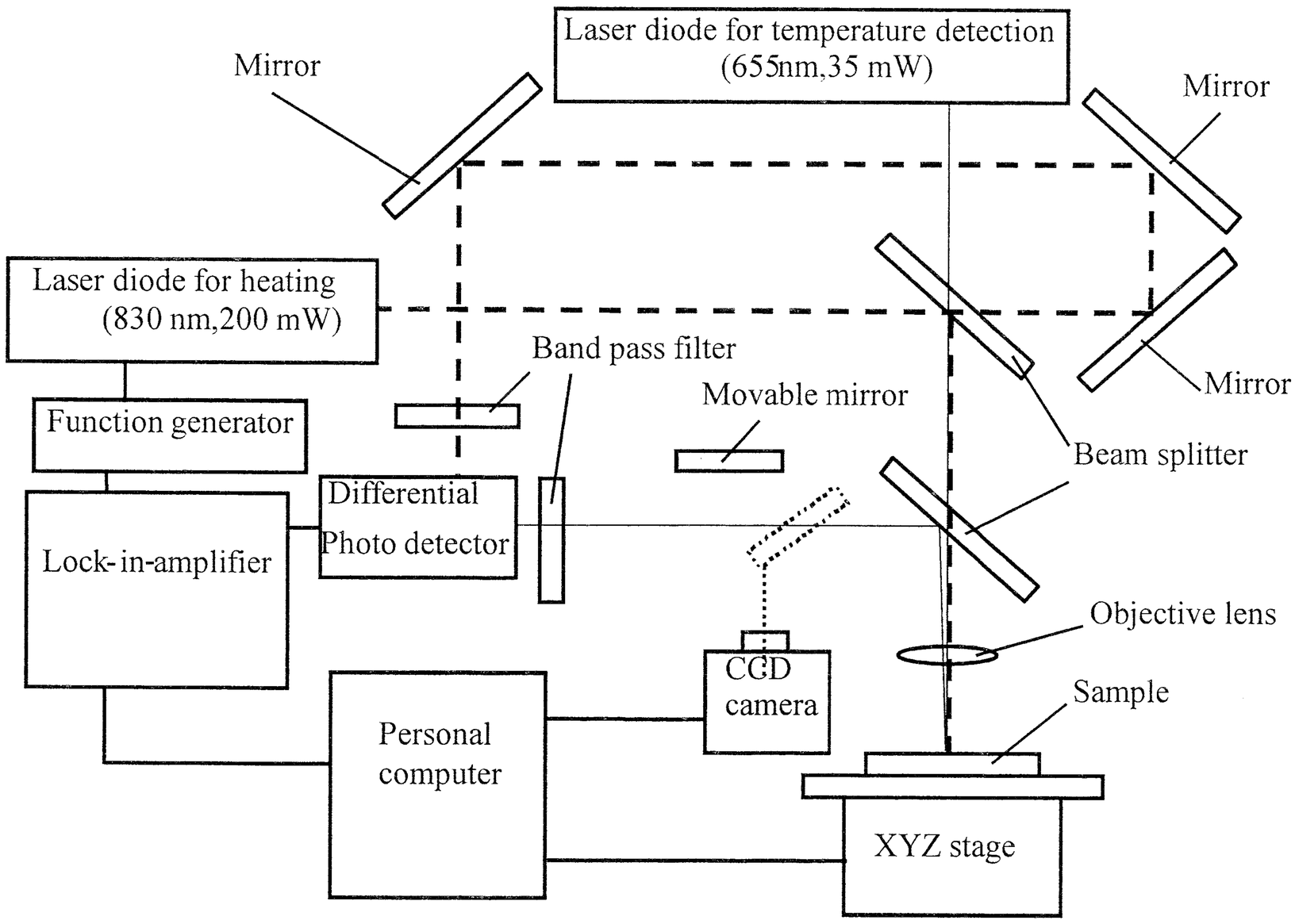

Fig. 2: Schematic diagram of the thermal microscope used in this study.

laser beam compared to the area used for reflectivity measurement to justify the use of one-dimensional heat transfer model in the analysis of the data obtained from measurement. The spatial resolution of the apparatus is estimated to be below 10 μm. The sample surface can be viewed using CCD camera built in the microscope optical system. The measurements are carried out at room temperature. Heating laser beam sinusoidal modulated with angular frequency ω is incident on the sample surface. The temperature response of the sample surface consequent to heat input from the laser is measured as the intensity variation of reflected beam of a second temperature sensing laser operated at constant energy. The temperature oscillates with a phase lag δ to the phase of heating laser. Thermal effusivity of the sample, b_s is derived using Eqs (2) to (4). The analytical formulation is based on the molybdenum coating-nitride sample two-layer system assuming that the contact thermal resistance of the coating/sample interface is negligible and the temperature distribution in the sample has reached a steady state. Analysis is based on one-dimensional heat flow in semi infinite layer.

$$\delta = \frac{3}{4}\pi + \arctan\left(\frac{\cosh^2 \sqrt{\frac{\omega\tau_m}{2}}}{\cos^2 \sqrt{\frac{\omega\tau_m}{2}}} \times \frac{\left(\tanh \sqrt{\frac{\omega\tau_m}{2}} + \beta \right)\left(\tanh \sqrt{\frac{\omega\tau_m}{2}} + \beta^{-1} \right)}{\left(\beta - \beta^{-1} \right) \tan \sqrt{\frac{\omega\tau_m}{2}}} \right) \quad (2)$$

$$\tau_m = d^2 / \alpha_m \quad (3)$$

$$\beta = b_s / b_m \quad (4)$$

where τ and d represent characteristic time for heat diffusion and thickness of a molybdenum layer, and the subscripts of s and m denote variables of the sample and the molybdenum layer, respectively.

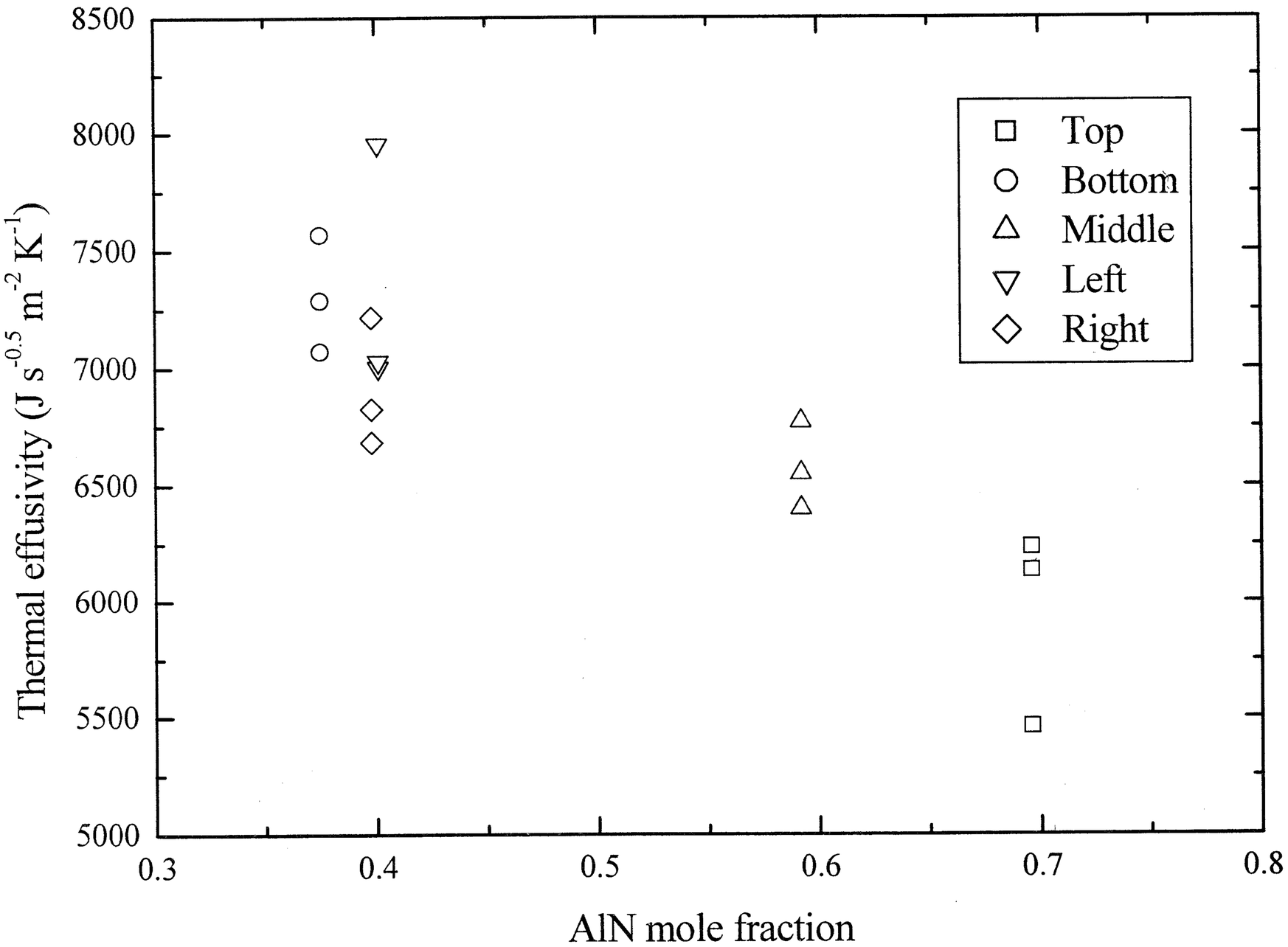

Fig. 3: Measured thermal effusivity of $Al_xGa_{1-x}N$ as a function of AlN mole fraction at room temperature.

The values of δ in Eq. (2) can be measured by using a lock-in amplifier. Thermophysical properties of the molybdenum layer (α_m, b_m) were experimentally determined separately. In addition, the thermal conductivity value λ_s of the sample can be estimated from b_s using Eq.(1) if the values for density, ρ and specific heat capacity, C_P are known.

3. RESULTS AND DISCUSSIONS

Figure 3 shows the thermal effusivity values obtained in this study as a function of AlN concentration. The thermal effusivity values are found to decrease with increasing AlN fraction in the alloy sample. Thermal conductivity, λ, of the sample was also estimated from the measured thermal effusivity, b, density, ρ, and specific heat capacity, Cp, using the relation;

$$\lambda = b^2 / \rho C_p \qquad (5)$$

The values of ρ and Cp for the $Al_xGa_{1-x}N$ samples were computed from those of pure AlN and GaN as follows;

$$\rho_{AlGaN} = W_{AlN} \times \rho_{AlN} + W_{GaN} \times \rho_{GaN} \qquad (6)$$

$$Cp_{AlGaN} = W_{AlN} \times C_{p\,AlN} + W_{GaN} \times C_{pGaN} \qquad (7)$$

where W in the mass fraction of each component nitride.

Density values for AlN and GaN at 300 K were taken from the literature /5, 19/. Molar heat capacity of AlN and GaN are given by Eq.(8) /5/ and Eq.(9) /20/ , respectively. Molar heat capacity is converted to specific heat capacity to derive values of Cp_{AlGaN} using eq.(7).

$$Cp_{AlN}=45.9+3.347\times10^{-3}\times T-14.98\times10^{5}\times T^{-2}\ \text{J/mol K} \qquad (8)$$

$$Cp_{GaN}=74.424-1.06\times10^{-3}\times T+46720\times T^{-2}-685.9\times T^{-0.5}\ \text{(J/ mol K)} \qquad (9)$$

The relevant values at 300 K derived from these equations and used in the present computation are summarized in **Table 2**.

Table 2

Thermal properties of GaN and AlN at 300 K.

	Specific Heat Capacity J $Kg^{-1}.K^{-1}$	Density Kg m^{-3}
GaN	404*	6150
AlN	689	3230

*From Jacob et al. /20/.

Other properties were taken from Ref.5 and 19.

The thermal conductivity values are plotted in **Figure 4**. The values measured at 300 K by Daly et al. /6/ and Liu and Balandin /7/ are also shown in **Figure 4** for comparison. The results obtained in this work are in the AlN fraction range between 0.38 and 0.70 and the thermal conductivity slightly decreases with increasing Al fraction. The thermal conductivities of pure GaN and AlN are 253 W/(m·K) /4/ and 285 W/(m·K) /5/, respectively. All the results of Daly et al. /6/ and Liu and Balandin /7/ are in the AlN fraction range below 0.45. Considering these results, the following comments may be made:

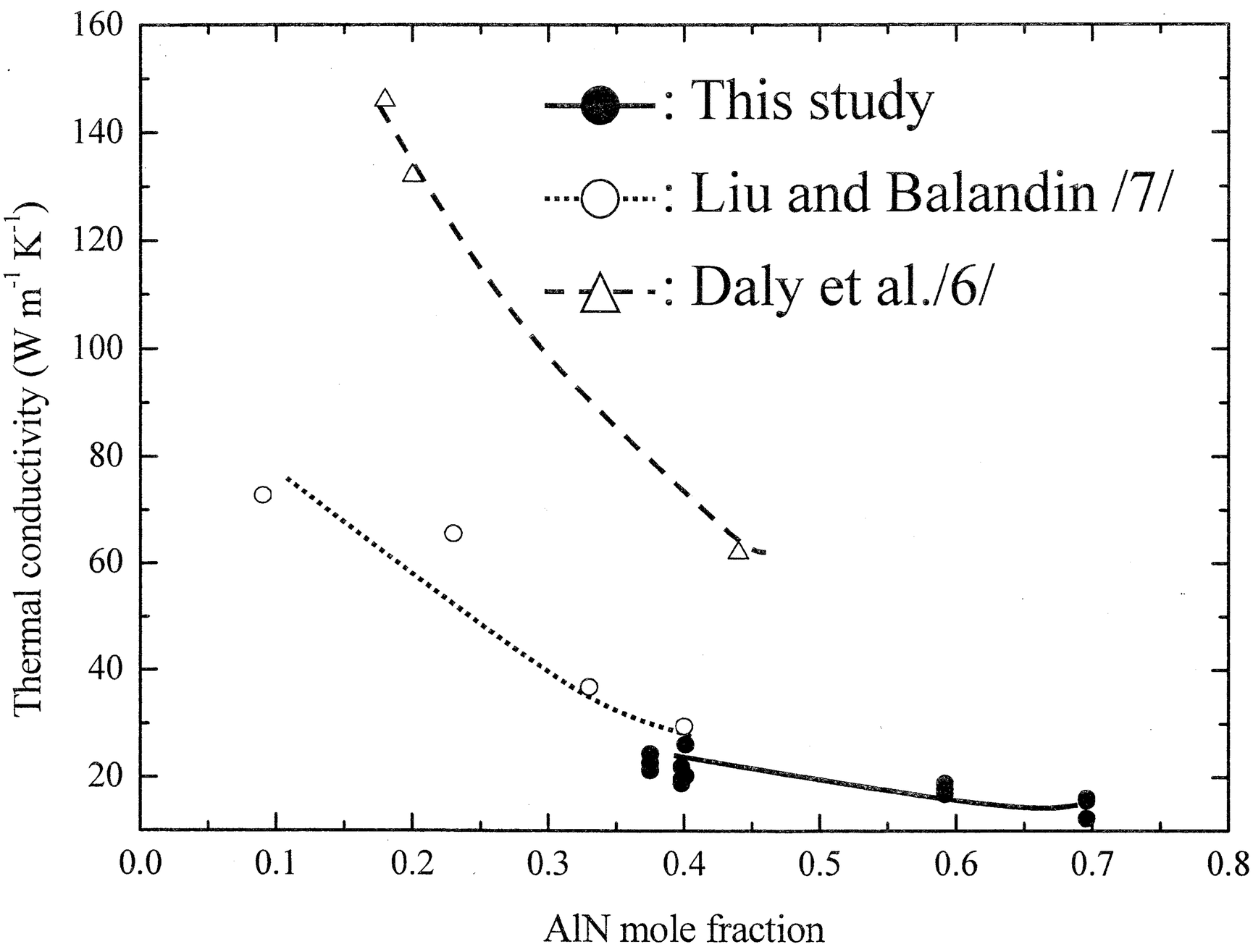

Fig. 4: Thermal conductivity of $Al_xGa_{1-x}N$ as a function of AlN mole fraction at room temperature.

1. Abrupt reduction of thermal conductivity is found when AlN fraction, x, increases from 0.0 to about 0.1.
2. The experimental data reported by Liu and Balandin /7/ are slightly higher than the results obtained in this study, but it is possible to connect the two sets of data to indicate the trend of variation of thermal conductivity with composition. On the contrary, the results of Daly et al. /6/ show the relatively large deviation from the values obtained in this work and those reported by Liu and Balandin /7/.
3. Based on the virtual crystal model, Liu and Balandin /7/ theoretically predicted that the thermal conductivity is close to a minimum at $x = 0.6$ by mixing GaN and AlN. The results of this study appear to support this and provide partial confirmation for the virtual crystal model. In this model, heat is mostly carried by acoustic phonons;

the electronic contribution to thermal conductivity is negligible. The acoustic phonons are scattered by the disorder perturbations and the anharmonity of the crystal. Future research should examine carefully the effect of impurities, defect and crystallinity $Al_xGa_{1-x}N$ alloys on transport properties.

4. CONCLUSION

The thermal effusivity and thermal conductivity of the $Al_xGa_{1-x}N$ alloy sample deposited on sapphire substrate have been successfully obtained by using a photothermal method in which temperature disturbance in the sample is generated through light absorption and light reflection is used to measure temperature. The potential of the thermal microscope for investigating thermal properties of very small region was also confirmed. The effect of AlN concentration on thermal effusivity and conductivity was examined at relatively higher AlN concentrations than in earlier studies. The compositional dependence of thermal conductivity obtained in this study and the earlier experimental data of by Liu and Balandin /7/ are consistent with the trend suggested by the virtual crystal model. However, preparative conditions may influence absolute values of thermal conductivity of alloys belonging to the $Al_xGa_{1-x}N$ system. For a more detailed discussion information on impurities, defects and crystallinity of the $Al_xGa_{1-x}N$ sample is required. Improvements to the thermal microscope and analysis of thermoreflectance data using a three-dimensional heat transfer model may also improve the quality of the data. In the meanwhile, the data obtained in this study can be used for modeling the performance of FETs using $Al_xGa_{1-x}N$ and avoiding problems related to overheating.

ACKNOWLEDGEMENTS

This work was supported by the Grant-in-aid (20656110) of the Ministry of Education, Culture, Sports, Science and Technology, Japan. The AlGaN wafer used for measurement was provided by Furukawa Co. Ltd., Japan. One of the authors (H.O.) acknowledges his appreciation of the collaborative effort to develop thermal microscope by N. Taketoshi, T. Baba, T. Yagi, H. Kato (from AIST: National Institute of Advanced Industrial Science and Technology, Tsukuba, Japan), K. Hatori, S. Kobayashi, K. Shinzato, K. Sakamoto, J. Saeki, T. Ohtuki and G. Matsui (from Bethel Corporation, Ishioka, Japan).

REFERENCES

1. A. Saura, H. Ji, K.P. Hilton, D.J. Wallis, M.J. Uren, T. Martin and M. Kuball, *IEEE Trans. Electron Devices*, **52**, (12), 3152-3158 (2007).
2. M. Kuball, S. Rajasingam, A. Saura, M.J. Uren, T. Martin, B.T. Hughes, K.P. Hilton and R.S. Balmer, *Appl. Phys. Lett.*, **82**, (1), 124-126 (2003).
3. N. Shigekawa, K. Onodera and K. Shiojima, *Jpn. J. Appl. Phy.*, **42**, 2245-2249(2003).
4. H. Shibata, Y. Waseda, H. Ohta, K. Kiyomi, K. Shimoyama, K .Fujito, H. Nagaoka, Y. Kagamitani, R. Simura and T. Fukuda, *Mater. Trans.*, **48**, (10), 2782-2786 (2007).
5. Y. Goldberg, *Properties of advanced semiconductor materials, GaN, AlN, InN, BN, SiC, SiGe* edited by M.E. Levinshtein, S.L. Rumyantsev and M.S. Shur, John Wiley & Sons, Inc., (2001), p.31-47.
6. B.C. Daly, H.J. Maris, A.V. Numikko, M. Kuball and J. Han, *J. Appl. Phys.*, **92**, (7), 3820-3824 (2002).
7. W. Liu and A.A. Balandin, *J. Appl. Phys.*, **97**, 073710-1-073710-6 (2005).
8. M. Clemens,C.A. Paddock and G. L. Eesley, *Phys. Rev. B*, **37**,1085 -1096 (1988).
9. H. Shjbata, H. Ohta. M. Miyashita, H. Noguchj, S. Sato, and Y. Waseda, *Bull. Adv. Mater. Process. IMRAM Tohoku University*, **58**,7-18 (2003).
10. R.M. Costescu, M.A. Wall, and D.G. Cahill, *Phys. Rev. B*, **67**, 054302, 1-5 (2003).
11. M. Kuwahara, O. Suzuki, N. Taketoshi, Y. Yamakawa, T. Yagi, P. J. Fons, K. Tsutsumi, M. Suzuki, T. Fukaya, J. Tominaga, and T. Baba, *Jpn. J. Appl. Phys.*, **45-2B**, 1419-1421 (2006).
12. N. Taketoshi, M. Ozawa, H. Ohta and T. Baba, *10th International Topical Meeting on Photoacoustic and Photothermal Phenomena, Rome, Italy,* (1998) ; *AIP*

Conference Proceedings **463** edited by F. Scudieri and M. Bertolotti, Woodbury, N.Y., (1999), p.315-317.

13. K. Hatori, T. Baba, N. Taketoshi and H. Ohta, *Rev. Sci. Inst.*, **76** , 114901-1-114901-7 (2005).
14. H. Fukuyama, T. Yoshimura, H. Yasuda and H. Ohta, *Int. J. Thermophys.*, **27**, 1760-1777 (2006).
15. S. Kume, I. Yamada, and K. Watari, *J. Am. Ceram. Soc.*, **92**, S153-S156 (2009).
16. S. Miyake, T. Kita, A. Miyake, K. Ikeda and H. Takamatsu, *Rev. Sci. Inst.*, **80**, 124901-1-124901-4 (2009).
17. I. Hatta , *Thermochim Acta*, **446**, 176-179 (2006).
18. N. Kuwano, Y. Kugiyama, Y. Nishikouri, T. Sato and A. Usui, *J. Crystal Growth*, **311**, 3085-3088 (2009).
19. Y. Bougrov, M. Levinshtein, S. Rumyantsev and A. Zubrilov, *Properties of advanced semiconductor materials, GaN, AlN, InN, BN, SiC, SiGe* edited by M.E. Levinshtein, S.L. Rumyantsev and M.S. Shur, John Wiley & Sons, Inc., (2001), p.1-30.
20. K.T. Jacob, S. Singh and Y. Waseda, *J. Mater. Res.*, **22**, 3475-3483 (2007).